JSSS
Journal of Sensors and Sensor Systems
Open Access

Moderate-temperature operable SO_2 gas sensor based on Zr^{4+} ion conducting solid electrolyte

Y. Uneme, S. Tamura, and N. Imanaka

Department of Applied Chemistry, Faculty of Engineering, Osaka University 2-1, Yamadaoka, Suita, Osaka
565-0871, Japan

Correspondence to: N. Imanaka (imanaka@chem.eng.osaka-u.ac.jp)

Abstract. A solid electrolyte type sulfur dioxide (SO_2) gas sensor that can operate at moderate temperatures was fabricated using Zr^{4+} ion conducting $Zr_{39/40}TaP_{2.9}W_{0.1}O_{12}$ solid electrolyte with $0.7La_2O_2SO_4 - 0.3(0.8Li_2SO_4 + 0.2K_2SO_4)$ having a large surface area and Zr metal as the auxiliary sensing electrode and reference electrode, respectively. Since the present sensor showed a quantitative, reproducible and rapid response which obeys the theoretical Nernst relationship even at 400 °C, it is a potential on site SO_2 gas sensing tool operable at moderate temperatures around 400 °C.

1 Introduction

Sulfur dioxide (SO_2) gas, emitted from sources such as incinerators and power stations, is a typical air pollutant causing acid precipitation. Consequently, reducing SO_2 gas emission into the atmosphere is important for environmental conservation. In order to effectively suppress SO_2 gas emission, it is essential to develop an SO_2 gas monitoring tool which can detect the gas rapidly and accurately at every emitting site. Currently, although there are analytical instruments that measure the SO_2 gas concentration based on chemical luminescence (Nakagawa et al., 1996) or infrared absorption (Frank and Meixner, 2001), these are not suitable for on site SO_2 gas monitoring because some pretreatment of the sample gas is required. Furthermore, these equipments are too expensive and too large to install at every emission site, and therefore, development of compact SO_2 gas sensors is necessary. Three types of compact SO_2 gas sensors have been proposed: solid electrolyte type (Maruyama et al., 1985; Yan et al., 1994), solid polymer electrolyte type (Chiou and Chou, 2002), and semiconductor type (Shimizu et al., 2001). Among these, the solid electrolyte type gas sensor is expected to be the most promising based on selectivity due to the unique characteristic of a solid electrolyte in which only single ion species can migrate in solids.

Recently, we have proposed a solid electrolyte type SO_2 gas sensor using the tetravalent Zr^{4+} ion conducting $Zr_{39/40}TaP_{2.9}W_{0.1}O_{12}$ (Imanaka et al., 2007) and the divalent O^{2-} ion conducting $(ZrO_2)_{0.92}(Y_2O_3)_{0.08}$ solid electrolytes with the $0.7La_2O_2SO_4 - 0.3(0.8Li_2SO_4 + 0.2K_2SO_4)$ solid as an auxiliary sensing electrode (Uneme et al., 2012). Although the previous sensor can detect SO_2 gas theoretically (obeying the Nernst equation over 2 months), a high operation temperature above 480 °C is required to obtain a stable and theoretical SO_2 response due to the high electrical resistance of the sensor cell and insufficient electrochemical reaction with the SO_2 gas at the auxiliary sensing electrode. The high operating temperature causes the sensing performance to deteriorate, and thus a lower operating temperature is required.

In this study, we designed a SO_2 gas sensor that can operate below 480 °C. Since the $(ZrO_2)_{0.92}(Y_2O_3)_{0.08}$ solid used as the reference electrode in the previous sensor shows considerably high electrical resistance below 500 °C, we replaced it with Zr metal. In addition, we improved the reactivity of the auxiliary sensing electrode. In order to achieve this, we enlarged the surface area of the auxiliary sensing electrode using polymethylmathacrylate (PMMA) as a template. Finally, the SO_2 gas sensing performance of the sensor was investigated at a moderate temperature of 400 °C.
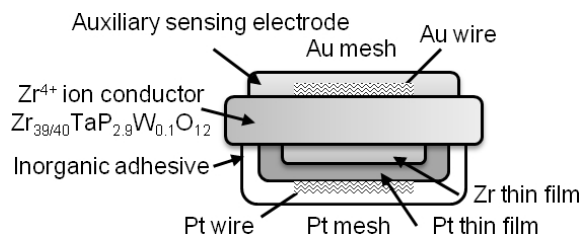
Figure 1. Schematic illustration of the SO$_2$ gas sensor based on the Zr^{4+} ion conducting solid electrolyte.

2   Experimental

Zr$_{39/40}$TaP$_{2.9}$W$_{0.1}$O$_{12}$ was synthesized by a solid state reaction. A stoichiometric mixture of ZrO(NO$_3$)$_2 \cdot$ 2H$_2$O, Ta$_2$O$_5$, (NH$_4$)$_2$HPO$_4$, and WO$_3$ was mixed using a ball milling apparatus (FRITSCH GmbH, P-7), and mixed powder was heated at 1200 °C for 12 h and 1300 °C for 12 h in air. The obtained powder was pelletized and sintered at 1300 °C for 12 h in air.

La$_2$O$_2$SO$_4$ was obtained by heating La$_2$S$_3$ at 1000 °C for 12 h in air. 0.7La$_2$O$_2$SO$_4 -$ 0.3(0.8Li$_2$SO$_4 +$ 0.2K$_2$SO$_4$) was prepared by mixing La$_2$O$_2$SO$_4$, Li$_2$SO$_4$ and K$_2$SO$_4$ at a stoichiometric ratio in an agate pot at a rotation speed of 300 rpm for 3 h using a planetary ball milling apparatus. The mixed powder was pelletized and sintered at 550 °C for 12 h in air.

Figure 1 shows a cross sectional view of the present SO$_2$ gas sensor. A Zr metal thin film as the reference electrode was loaded on the sintered Zr$_{39/40}$TaP$_{2.9}$W$_{0.1}$O$_{12}$ pellet and subsequently covered with a Pt thin film by ion beam sputtering (Elionix, ESC-101). Au and Pt meshes were attached on the Zr$_{39/40}$TaP$_{2.9}$W$_{0.1}$O$_{12}$ and Zr reference electrode as current collectors. To form the auxiliary sensing electrode, a mixture of 0.7La$_2$O$_2$SO$_4 -$ 0.3(0.8Li$_2$SO$_4 +$ 0.2K$_2$SO$_4$) and polymethylmethacrylate (PMMA, 0.6–1.0 μm in diameter) was attached on the Au mesh and then heated at 500 °C for 1 h in air to remove PMMA. The SO$_2$ gas sensing performance was investigated at 400 °C. SO$_2$ gas concentrations from 500 to 3000 ppm were regulated by mixing pure SO$_2$ with N$_2$ and O$_2$, and the total gas flow rate was kept constant at 100 ml min^{-1} with the O$_2$ gas pressure (PO$_2$) fixed at 0.21 atm. The sensor Electromotive force (EMF) output was measured using a digital electrometer (Advantest, R8240). The morphology of the auxiliary sensing electrodes was characterized by scanning electron microscopy (SEM) (Shimadzu, SS-550). The specific surface area of the auxiliary sensing electrodes was measured using the Brunauer-Emmett-Teller (BET) method by nitrogen adsorption at -196 °C (Micromeritics Tristar 3000).

3   Results and discussion

Figure 2 shows the SEM images of the auxiliary sensing electrode on the Zr$_{39/40}$TaP$_{2.9}$W$_{0.1}$O$_{12}$ solid electrolyte. Large pores were observed for 0.7La$_2$O$_2$SO$_4 -$ 0.3(0.8Li$_2$SO$_4 +$
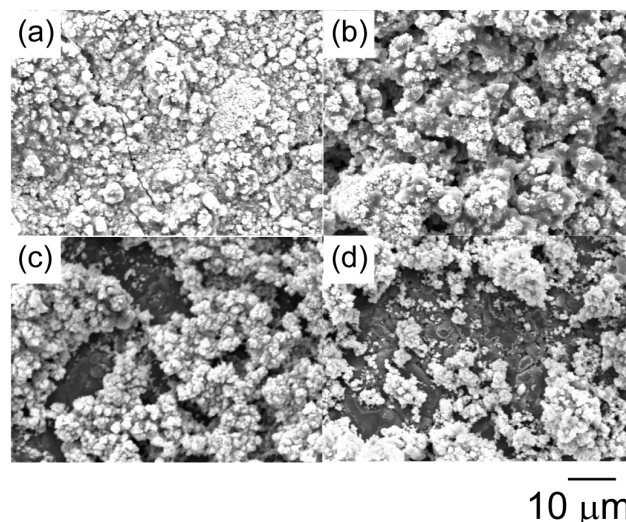

Figure 2. SEM images of the auxiliary sensing electrodes obtained by heating 0.7La$_2$O$_2$SO$_4 -$ 0.3(0.8Li$_2$SO$_4 +$ 0.2K$_2$SO$_4$) with **(a)** 0 wt %, **(b)** 10 wt %, **(c)** 30 wt %, or **(d)** 50 wt % PMMA on the Zr$_{39/40}$TaP$_{2.9}$W$_{0.1}$O$_{12}$ solid electrolyte.

0.2K$_2$SO$_4$) with 10 wt % PMMA, while 0.7La$_2$O$_2$SO$_4 -$ 0.3(0.8Li$_2$SO$_4 +$ 0.2K$_2$SO$_4$) without PMMA was sintered well. Furthermore, it was confirmed that the specific surface area of 0.7La$_2$O$_2$SO$_4 -$ 0.3(0.8Li$_2$SO$_4 +$ 0.2K$_2$SO$_4$) with 10 wt % PMMA (1.3849 m^2 g^{-1}) was considerably larger than that of 0.7La$_2$O$_2$SO$_4 -$ 0.3(0.8Li$_2$SO$_4 +$ 0.2K$_2$SO$_4$) without PMMA (0.4897 m^2 g^{-1}). From these results, it was concluded that evaporation of PMMA during the heat treatment resulted in pore formation in the auxiliary sensing electrode. On the other hand, when a large amount of PMMA over 10 wt % was mixed with 0.7La$_2$O$_2$SO$_4 -$ 0.3(0.8Li$_2$SO$_4 +$ 0.2K$_2$SO$_4$) solid, the surface of the Zr$_{39/40}$TaP$_{2.9}$W$_{0.1}$O$_{12}$ solid was clearly seen under the auxiliary sensing electrode due to the formation of big pores. Since reduction in the contact area between Zr$_{39/40}$TaP$_{2.9}$W$_{0.1}$O$_{12}$ (solid electrolyte) and 0.7La$_2$O$_2$SO$_4 -$ 0.3(0.8Li$_2$SO$_4 +$ 0.2K$_2$SO$_4$) (auxiliary sensing electrode) causes deterioration of the ion exchange reaction (described below), we selected 0.7La$_2$O$_2$SO$_4 -$ 0.3(0.8Li$_2$SO$_4 +$ 0.2K$_2$SO$_4$) with 10 wt % PMMA as the auxiliary sensing electrode.

Figure 3 shows the representative sensor response curves measured by the sensors using auxiliary sensing electrodes with 10 wt % PMMA and without PMMA for SO$_2$ gas concentrations from 500 to 3000 ppm at 400 °C. Although both sensors showed stable sensor EMF output without electrical noise even at 400 °C (the electrical resistance of the sensor cell was reduced using the Zr metal as a reference electrode), the response time, which is defined as the time to attain 90 % total sensor EMF output change, was considerably different. For the sensor using the auxiliary sensing electrode with 10 wt % PMMA, the response time was ca. 4 min, which is shorter than that for the sensor using
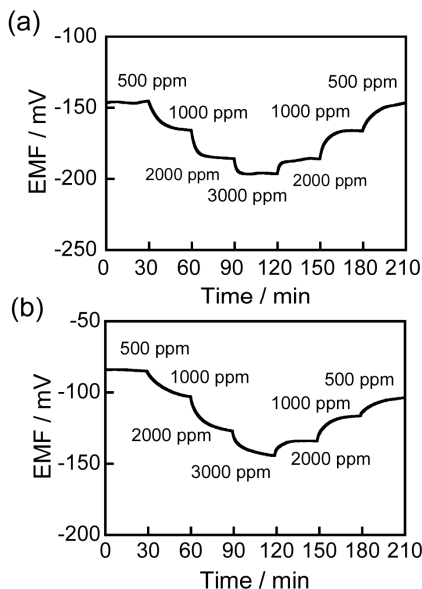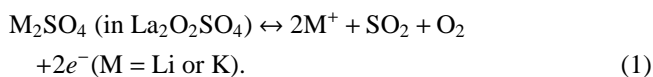
(a)

(b)

Figure 3. Representative sensor response curves measured by the sensors using the auxiliary sensing electrodes **(a)** with and **(b)** without 10 wt % PMMA for SO₂ gas concentrations between 500 to 3000 ppm at 400 °C.
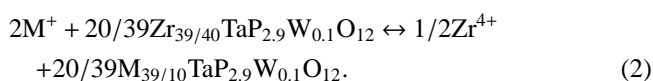
the auxiliary sensing electrode without PMMA (ca. 20 min). In addition, the sensor using the auxiliary sensing electrode with 10 wt % PMMA showed the same sensor EMF output for each SO₂ gas concentration in increasing and in decreasing processes, while the sensor EMF outputs for decreasing SO₂ gas concentration were lower than those for increasing concentration for the sensor using the auxiliary sensing electrode without PMMA. This is because the reactivity of the rate-limiting reaction between the auxiliary sensing electrode and SO₂ gas was improved by the increasing surface area of $0.7La_2O_2SO_4 - 0.3(0.8Li_2SO_4 + 0.2K_2SO_4)$.

The following reactions were proposed to occur at the $0.7La_2O_2SO_4 - 0.3(0.8Li_2SO_4 + 0.2K_2SO_4)$ auxiliary sensing electrode, at the interface between the auxiliary sensing electrode and $Zr_{39/40}TaP_{2.9}W_{0.1}O_{12}$ solid electrolyte, and at the Zr metal thin film reference electrode.

At the auxiliary sensing electrode:

$$M_2SO_4 \text{ (in } La_2O_2SO_4) \leftrightarrow 2M^+ + SO_2 + O_2$$
$$+2e^- (M = Li \text{ or } K). \tag{1}$$

At the interface between the auxiliary sensing electrode and solid electrolyte:

$$2M^+ + 20/39Zr_{39/40}TaP_{2.9}W_{0.1}O_{12} \leftrightarrow 1/2Zr^{4+}$$
$$+20/39M_{39/10}TaP_{2.9}W_{0.1}O_{12}. \tag{2}$$

At the reference electrode:

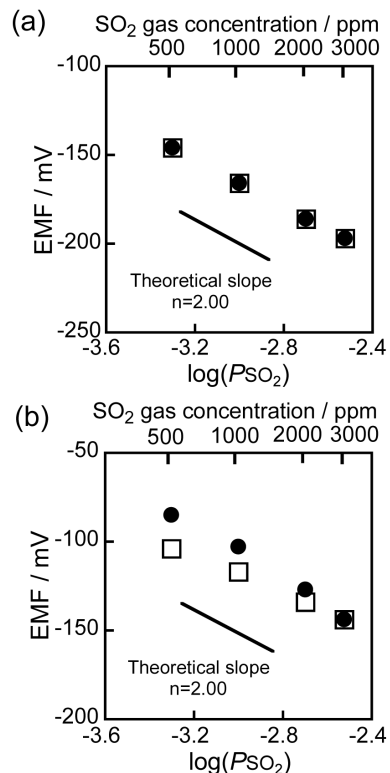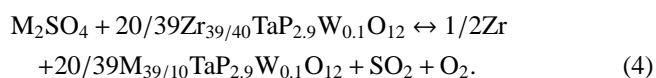$$1/2Zr^{4+} + 2e^- \leftrightarrow 1/2Zr. \tag{3}$$

(a)

(b)

Figure 4. Relationship between the sensor EMF output and log(PSO₂) for the sensors using the auxiliary sensing electrodes **(a)** with and **(b)** without 10 wt % PMMA. ● and □ represent the sensor EMF outputs with increasing and decreasing SO₂ gas concentrations, respectively. The solid line shows the theoretical slope estimated from the Nernst equation.

From Eqs. (1)–(3), the total chemical reaction and the following Nernst equation can be written as

$$M_2SO_4 + 20/39Zr_{39/40}TaP_{2.9}W_{0.1}O_{12} \leftrightarrow 1/2Zr$$
$$+20/39M_{39/10}TaP_{2.9}W_{0.1}O_{12} + SO_2 + O_2. \tag{4}$$

$$E = E_0 + (RT/nF)\ln\left\{(aZr)^{-1/2} \cdot (aM_{39/10}TaP_{2.9}W_{0.1}O_{12})^{-20/39}\right.$$
$$\left. \cdot (PSO_2)^{-1} \cdot (PO_2)^{-1} \cdot (aM_2SO_4) \cdot (aZr_{39/40}TaP_{2.9}W_{0.1}O_{12})^{20/39}\right\} \tag{5}$$

Here, R, F, and n are, respectively, the gas constant, the Faraday's constant, and the number of electrons participating in the SO₂ gas sensing (here, $n = 2.00$). a and P are, respectively, the activity of the solid materials and partial pressure of the gas species. Since the activities of the solid materials (i.e., Zr, $M_{39/10}TaP_{2.9}W_{0.1}O_{12}$, M_2SO_4, and $Zr_{39/40}TaP_{2.9}W_{0.1}O_{12}$) are strictly constant if the temperature is fixed, and the oxygen partial pressure (PO_2) was maintained at 0.21 atm during the measurement, Eq. (5) can be simplified to

$$E = C(\text{constant}) - (RT/nF)\ln(PSO_2)(n = 2.00). \tag{6}$$

Figure 4 shows the relationship between the sensor EMF output and the logarithm of the SO₂ gas concentration. The

theoretical slope ($n = 2.00$) estimated from Eq. (6) is shown as a solid line. For the sensor using the auxiliary sensing electrode with 10 wt % PMMA, the n values estimated from the slopes for the increasing and decreasing SO$_2$ gas concentrations were both 2.03, which coincided well with the theoretical value ($n = 2.00$). This indicates that the sensor using the auxiliary sensing electrode with 10 wt % PMMA shows a theoretical response for SO$_2$ gas at operating temperatures as low as 400 °C. In contrast, for the sensor using the auxiliary sensing electrode without PMMA, the n values were, respectively, 1.77 and 2.58 for the increasing and decreasing SO$_2$ gas concentrations. The differences between these values and the theoretical value are due to the lower reactivity of the auxiliary sensing electrode caused by the smaller surface area. Furthermore, the sensor EMF output of the sensor using the auxiliary sensing electrode without PMMA was higher than that of the sensor using the auxiliary sensing electrode with 10 wt % PMMA. The reason for the difference in sensor EMF output was considered to be by partial oxidation of the reference electrode. Although Zr metal was covered with Pt sputtered film to prevent the oxidation of Zr metal, ZrO$_2$ might be partially formed in the reference electrode, resulting in the change of the sensor EMF output.

4   Conclusions

A SO$_2$ gas sensor that can operate at moderate temperatures was fabricated using the Zr^{4+} ion conducting Zr$_{39/40}$TaP$_{2.9}$W$_{0.1}$O$_{12}$ solid electrolyte with the $0.7\mathrm{La_2O_2SO_4} - 0.3(0.8\mathrm{Li_2SO_4} + 0.2\mathrm{K_2SO_4})$ solid and the Zr metal thin film as an auxiliary sensing electrode and a reference electrode, respectively. By applying Zr metal that has low electrical resistance and an auxiliary sensing electrode with a large surface area, the present SO$_2$ gas sensor showed a continuous, reproducible, and theoretical response even at the operating temperature of 400 °C.

References

Chiou, C. Y. and Chou, T. C.: Amperometric SO$_2$ gas sensors based on solid polymer electrolytes, Sensor. Actuat. B-Chem., 87, 1–7, 2002.

Frank, J. and Meixner, H.: Sensor system for indoor air monitoring using semiconducting metal oxides and IR-absorption, Sensor. Actuat. B-Chem., 78, 298–302, 2001.

Imanaka, N., Tamura, S., and Itano, T.: Extraordinarily high Zr^{4+} ion conducting solid, J. Am. Chem. Soc., 129, 5338–5339, 2007.

Maruyama, T., Saito, Y., Matsumoto, Y., and Yano, Y.: Potentiometric sensor for sulfur oxides using Nasicon as a solid electrolyte, Solid State Ionics, 17, 281–286, 1985.

Nakagawa, N., Kawabata, S., Nishiyama, K., Utsunomiya, K., Yamamoto, I., Wada, T., Yamashita, Y., and Yamashita, N.: Analytical detection system of mixed odor vapors using chemiluminescence-based gas sensor, Sensor. Actuat. B-Chem., 34, 334–338, 1996.

Shimizu, Y., Matsunaga, N., Hyodo, T., and Egashira, M.: Improvement of SO$_2$ sensing properties of WO$_3$ by noble metal loading, Sensor. Actuat. B-Chem., 77, 35–40, 2001.

Uneme, Y., Tamura, S., and Imanaka, N.: Sulfur Dioxide Gas Sensor Based on Zr^{4+} and O^{2-} Ion Conducting Solid Electrolytes with Lanthanum Oxysulfate as an Auxiliary Sensing Electrode, Sensor. Actuat. B-Chem., in press, 2012.

Yan, Y., Shimizu, Y., Miura, N., and Yamazoe, N.: High performance solid electrolyte SO$_X$ sensor using MgO stabilized zirconia tube and Li$_2$SO$_4$-CaSO$_4$-SiO$_2$ auxiliary phase, Sensor. Actuat. B-Chem., 20, 81–87, 1994.